Hydroclimatic Trends in the Mississippi River Basin from 1948 to 2004

TAOTAO QIAN, AIGUO DAI, AND KEVIN E. TRENBERTH

National Center for Atmospheric Research, Boulder, Colorado*

(Manuscript received 11 September 2006, in final form 18 January 2007)

ABSTRACT

The trends of the surface water and energy budget components in the Mississippi River basin from 1948 to 2004 are investigated using a combination of hydrometeorological observations and observation-constrained simulations of the land surface conditions using the latest version of the Community Land Model version 3 (CLM3). The atmospheric forcing data for the CLM3 were constructed by adding the intramonthly variations from the 6-hourly National Centers for Environmental Prediction–National Center for Atmospheric Research (NCEP–NCAR) reanalysis to observation-based analyses of monthly precipitation, surface air temperature, and cloud cover. The model-based analysis suggests that, for the surface water budget, the observed increase in basin-averaged precipitation is compensated by increases in both runoff and evapotranspiration. For the surface energy budget, the decrease of net shortwave radiation associated with observed increases in cloudiness is compensated by decreases in both net longwave radiation and sensible heat flux, while the latent heat flux increases in association with wetter soil conditions. Both the simulated surface water and energy budgets support the view that evapotranspiration has increased in the Mississippi River basin from 1948 to 2004. Sensitivity experiments show that the precipitation change dominates the evapotranspiration trend, while the temperature and solar radiation changes have only small effects. Large spatial variations within the Mississippi River basin and the contiguous United States are also found. However, the increased evapotranspiration is ubiquitous despite spatial variations in hydrometeorology.

1. Introduction

Global surface temperatures have increased between 0.4° and 0.8°C since the late nineteenth century (Houghton et al. 2001), and the associated changes in the earth's energy balance are likely to affect other climatic factors such as the components of the terrestrial water cycle (Huntington 2006; Margulis et al. 2006). The partitioning of surface energy between sensible heating and evaporative cooling plays an important role in land–atmosphere interactions and climate change (Koster et al. 2004; Seneviratne et al. 2006). Actual evaporation, or more generally evapotranspiration (referred to as E hereafter), is constrained at the land surface by the energy and water budgets. The simplified land surface energy budget has five components: net shortwave or solar radiation, net longwave radiation, latent heat flux, sensible heat flux, and heat flux into the ground. The surface water budget over land includes four components: precipitation, evapotranspiration, runoff, and the change of soil and groundwater content. Historical records generally exist only for the solar radiation, precipitation, and runoff (discussed below), but not for the other components. In previous studies, the incomplete observations of these two budgets have led to conflicting estimates of the trends in actual evapotranspiration over global land, including the United States (see review by Huntington 2006).

For the energy budget, observations show that over most of the United States, total cloud cover has been increasing (Karl and Steurer 1990; Sun 2003; Groisman et al. 2004; Dai et al. 2006), leading to decreases in surface downward solar radiation (Gilgen et al. 1998; Liepert 2002). Another indirect indicator of increased cloud and reduced surface solar radiation is the observed decrease in diurnal temperature range (DTR) over many land areas, including the United States from

* The National Center for Atmospheric Research is sponsored by the National Science Foundation.

Corresponding author address: Dr. Taotao Qian, Climate and Global Dynamics Division, National Center for Atmospheric Research, P.O. Box 3000, Boulder, CO 80307.
E-mail: tqian@ucar.edu

DOI: 10.1175/JCLI4262.1

1950 to the 1990s (Easterling et al. 1997), because clouds reduce surface solar heating and thus daytime maximum temperature (Dai et al. 1999). There are no direct observations of actual evapotranspiration except for a few sites such as the Atmospheric Radiation Measurement/Cloud and Radiation Testbeds (ARM/CART), the Oklahoma Mesonet, and some Russian sites with tower flux measurements or short-term field experiments, and the FLUXNET measurements (Baldocchi et al. 2001) only for the recent period, but an indirect observation—pan evaporation (E_{pan}), which is the evaporation from the open water surface of an evaporation pan—has shown decreasing trends from the 1950s or 1960s to the 1990s over the United States and parts of Europe and Siberia (Peterson et al. 1995), India (Chattopadhyay and Hulme 1997), and China (Thomas 2000; Liu et al. 2004). The decreases in pan evaporation are physically consistent with decreased solar radiation (Roderick and Farquhar 2002) associated with observed increases in cloud cover (Dai et al. 1997a, 1999) or associated with increased aerosols and other air pollutants (Stanhill and Cohen 2001; Liu et al. 2004) that have changed the optical properties of the atmosphere, in particular those of clouds. The surface latent heat flux is directly proportional to evapotranspiration.

Based on the pan observations, Peterson et al. (1995) concluded that actual evapotranspiration over the United States and former Soviet Union may have decreased from the 1950s to the 1990s because of reduced surface heating. However, this is inconsistent with the observed temperature increases in these areas. Based on theoretical deductions, Brutsaert and Parlange (1998) concluded that actual evapotranspiration should be negatively correlated with pan evaporation over regions with less than adequate moisture. Over northern extratropical land areas actual evapotranspiration may have increased due to increases in precipitation (e.g., Dai et al. 1997b) and higher temperatures (e.g., Jones and Moberg 2003), and thus the hydrological cycle may have intensified.

Further analyses suggest increasing trends in actual evapotranspiration over the United States and Russia during the period from the 1950s to the 1990s (Lawrimore and Peterson 2000; Golubev et al. 2001), and they support Brutsaert and Parlange's (1998) interpretation. Using parallel observations of actual evapotranspiration and pan evaporation at five Russian experimental sites, Golubev et al. (2001) developed a method to estimate actual evapotranspiration from pan evaporation measurements and showed an actual evapotranspiration increase over most dry regions of Russia from 1951 to 1987 and the United States from 1957 to 1998, and a humid region at the northwestern tip of the western United States from 1961 to 1998. Only over the heavily forested regions of Russia (1951–90) and the southeastern United States (1957–98) did they find a decrease in actual evapotranspiration.

Based primarily on observations of net radiation over at least a decade from sparse locations over land (predominantly over northern extratropical land), Wild et al. (2004) estimated that there has been a reduction in net radiative heating at the surface on the order of 1–28 W m^{-2} $century^{-1}$ between 1960 and 1990. Given the observed surface warming, they inferred a decrease of evaporative cooling over global land (assuming little change in sensible heating) during the same period. However, because sensible heat change is not negligible, their inference is not justified. Milly and Dunne (2001) deduced a large negative trend in the sensible heat flux (–11 W m^{-2} $century^{-1}$) over the Mississippi basin from 1949 to 1997 through semiempirical water balance theory and energy budget analyses.

Since evapotranspiration occurs mainly during midday with solar heating as the driving force, decreases in solar radiation could reduce evapotranspiration, although changes in soil moisture due to precipitation changes may play a more important role over many land areas. In other words, it is necessary to also consider the surface water budget to determine evapotranspiration trends over most land areas.

For the water budget, observations show that precipitation increased over northern mid- and high-latitude land areas during the twentieth century (e.g., Dai et al. 1997b). Over most of the United States, historical records show that both precipitation (P) and streamflow or runoff (R) increased during the past 50–100 yr (e.g., Karl and Knight 1998; Groisman et al. 1999; Lettenmaier et al. 1999; Lins and Slack 1999; Kunkel et al. 1999; McCabe and Wolock 2002; Groisman et al. 2001, 2004), and $P - R$ has also increased (Milly and Dunne 2001; Walter et al. 2004). Ignoring long-term changes in land water storage, Walter et al. (2004) inferred, based on the $P - R$ trend, that evapotranspiration increased over major U.S. river basins during the last 50 yr. Based primarily on observed precipitation and streamflow and using mass balance, Milly and Dunne (2001) deduced an increasing trend in actual evapotranspiration over the Mississippi River basin during 1949–97.

In summary, although there is still some controversy about the evapotranspiration trend (e.g., Ohmura and Wild 2002; Wild et al. 2004), the weight of evidence supports an increasing trend in evapotranspiration over the United States. The controversy mainly arises from incomplete observations of the energy and water bud-

gets, which further hinders our understanding of the physical mechanisms of evapotranspiration changes. In this study, a comprehensive evaluation of historical changes in these two budgets using available observational data and observation-constrained land model simulations is made. Our goal is to provide a self-consistent analysis of the changes in surface water and energy fluxes over the United States during 1948–2004, with a focus on the Mississippi River basin where long-term records of streamflow provide additional constraints on the analysis. Because of incomplete observations of surface water and energy fields, we employ a comprehensive land surface model, namely the Community Land Model version 3 (CLM3), forced with observation-based precipitation, temperature, and other atmospheric forcing to simulate historical land surface conditions. The CLM3 simulations provide complementary information for evapotranspiration, soil moisture, and surface energy fluxes that are physically consistent with available hydroclimatic records. They also provide a means to examine sensitivities of surface evapotranspiration and other fluxes to individual atmospheric forcing (e.g., precipitation and temperature). Combining the CLM3 simulations with historical data of temperature, precipitation, cloudiness, and streamflow allows us to provide a full assessment of hydroclimatic changes over the Mississippi River basin during 1948–2004.

2. Data and analysis methods

Monthly observational data over the United States from 1948 to 2004 are available for surface air temperature from the Climate Research Unit (CRU; Jones and Moberg 2003), precipitation (Chen et al. 2002), streamflow (Dai and Trenberth 2002), cloud cover (Mitchell et al. 2004; Dai et al. 2006), and diurnal temperature range [from the Global Historical Climatology Network version 2 (GHCN2); Peterson and Vose 1997]. Relatively short records of surface solar radiation from a limited number of stations were available over the United States (Liepert 2002), but we used them only to evaluate the cloudiness-adjusted solar radiation (Qian et al. 2006). Short records of soil moisture from Illinois were also used only to evaluate the CLM3 simulations (Qian et al. 2006).

The historical records of monthly streamflow of the Mississippi River basin are from gauge measurements at Vicksburg, Mississippi (Dai and Trenberth 2002). The record extends only to September 1998. The measurements of gauge height were continually recorded and are highly correlated with streamflow (r = 0.96 for monthly data). The daily historical data of gauge height (0800 CST reading) of 1947–2004 (from http://rivergages.com/, which is maintained by the U.S. Army Corps of Engineers) were used. A linear regression analysis of the monthly streamflow and gauge height for October 1947−September 1998 was performed and then used to derive monthly streamflow after September 1998 from the gauge height data.

To complement the available observational data and for sensitivity analyses, the CLM3 was used to simulate the historical land surface conditions driven by observation-constrained atmospheric forcing (Qian et al. 2006). The CLM3 is a comprehensive land surface model designed for use in coupled climate system models (Dai et al. 2003; Oleson et al. 2004). The CLM3 simulates all major land surface processes. They include 1) vegetation composition, structure, and phenology; 2) absorption, reflection, and transmittance of solar radiation; 3) absorption and emission of longwave radiation; 4) momentum, sensible heat, and latent heat (ground and canopy evaporation; plant transpiration) fluxes; 5) heat transfer in soil and snow; 6) canopy hydrology; 7) snow hydrology; 8) soil hydrology (surface runoff, infiltration, subsurface drainage, and redistribution of water within the 10-layer column, which has a fixed depth of 3.43 m); 9) stomatal physiology and photosynthesis; and 10) routing of surface runoff to the oceans. The CLM3 was run over global land from 1948 to 2004 (after spinup, see Qian et al. for details) at T42 (~2.8°) resolution with the spatial heterogeneity of land surface represented as a nested subgrid hierarchy in which grid cells are composed of multiple land units, snow/soil columns, and plant functional types.

The focus of this paper is the long-term (57-yr) trend of water and energy budgets averaged over the whole Mississippi River basin (2 896 000 km^2), not the small-scale variability. For this purpose, we used the global forcing dataset at T62 (~1.8°) resolution described by Qian et al. (2006). It was derived by combining long-term variations from monthly time series of observed precipitation, surface air temperature, and other climate records with the short-term (intramonthly) variations contained in the National Centers for Environmental Prediction–National Center for Atmospheric Research (NCEP–NCAR) reanalysis (Kalnay et al. 1996) for a 57-yr period (1948–2004) over global land areas. We also used the 40-yr European Centre for Medium-Range Weather Forecasts (ECMWF) Re-Analysis (ERA-40) data (1958–2001) for the intramonthly variability. The results showed that the intramonthly variability from both NCEP–NCAR and ERA-40 make no significant differences to the CLM3-simulated long-term trends. Although some long-term simulations have used the NCEP–NCAR reanalysis data directly as atmospheric forcing (e.g., Fan et al. 2006), this was not

done here owing to spurious trends and biases (mainly before the 1970s). Instead, as given by Qian et al. (2006), the NCEP–NCAR reanalysis was used to only provide the high-frequency information. Recently, the North American Regional Reanalysis (NARR; 1979–2003; Mesinger et al. 2006) was released and provides much higher spatial resolution and improved precipitation fields compared with the global NCEP–NCAR reanalysis. However it is not global, as is required for our simulations. Also, its length of record is too short for long-term trend analyses. This also applies to many other model-assimilated land surface data, for example, the Global Soil Wetness Project (GSWP; Dirmeyer et al. 1999) and the Global Land Data Assimilation System (GLDAS; Rodell et al. 2004). Further, some problems have been identified in the NARR (e.g., in evaporation fields: see Nigam and Ruiz-Barradas 2006). We have performed test runs at 0.5° resolution for comparison with those at T42 (~2.8°) with the CLM3 and results show that large-scale (>500 km) variations are very similar.

For observational precipitation, the Chen et al. (2002) dataset (for 1948–96) supplemented by the GPCP v2 data (Adler et al. 2003) for 1997–2004 was chosen because Chen et al. used a large network of raingauges in creating the climatological mean fields, while the GPCP has better gauge coverage than the Chen et al. data after 1997. Monthly surface air temperatures were derived by adding the temperature anomalies from Jones and Moberg (2003) to the climatology of New et al. (1999). Surface downward solar radiation from the reanalysis was adjusted, first, for variations and trends using gridded monthly cloud cover anomalies derived from surface observations (Mitchell et al. 2004) merged with the latest synoptic observations (see Dai et al. 2006) and, second, for mean biases using satellite observations during July 1983–June 2001. Because observational analyses of surface specific humidity for 1948–2004 are unavailable and the reanalysis relative humidity (RH) (constrained by lower-tropospheric radiosonde data) is highly correlated with synoptic humidity observations from Dai (2006), we used the surface RH from the reanalysis to derive the specific humidity with the adjusted air temperature. Surface wind speed and air pressure were interpolated directly from the 6-hourly reanalysis data to 3-hourly resolution (see Qian et al. 2006).

The CLM3 simulations were evaluated with available data on soil moisture and streamflow from the world's major rivers in Qian et al. (2006). The CLM3 successfully reproduces the observed time series of river outflow from most of the world's top 200 rivers. This includes the Mississippi River, with a correlation coefficient (r) of 0.94 (the mean bias is 96.1 $km^3\ yr^{-1}$ or 17.4% of the observed mean). It also captures the year-to-year variations in the few locations with observed soil moisture content over Illinois ($r = 0.73$) and several Eurasian regions ($r = 0.56$ to 0.73).

To perform areal averaging and integration and to obtain estimates over drainage areas for individual river basins, a database for the world river network is needed. The simulated river database STN-30p (Vörösmarty et al. 2000), a global simulated topological network at 30′ spatial resolution, was used. The observed runoff for the Mississippi River basin was estimated by dividing the station streamflow at Vicksburg, Mississippi, by the drainage area upstream (2 896 000 km^2).

Although the CLM3 simulations are on a T42 (about 2.8°) Gaussian grid, the outputs were first regridded onto a rectangular grid (2.5° × 2.5°) using bilinear interpolation and then to the 0.5° × 0.5° grid by simply assigning all subgrid boxes to the value of the low-resolution box. The basin areal averaging is then performed on the 0.5° × 0.5° grid using the STN-30p river database. The annual means of all the variables in this study are for the water year (1 October of the previous year to 30 September of the year). This interval is used because hydrological systems are typically at their lowest levels near 1 October in the Northern Hemisphere.

We analyze both the surface water and energy budgets. The simplified surface water budget over land can be written as

$$dW/dt = P - E - R. \tag{1}$$

The temporal change of land water storage dW/dt (which includes soil liquid and ice water, snow water, and canopy water) is equal to precipitation (P) minus evapotranspiration (E) and runoff (R) (which includes the surface and subsurface flow). The human influences through consumptive water use and filling of reservoirs and depletion of groundwater are discussed in Milly and Dunne (2001), and they are excluded in our analyses here. In the water budget, precipitation and runoff are from observations. The observation-constrained CLM3-simulated evaporation, runoff, and change of land water storage are used to complement the available observational data.

The simplified surface energy budget can be written as

$$G = \mathrm{SW} - \mathrm{LW} - \mathrm{SH} - \mathrm{LH}, \tag{2}$$

where these terms are the net shortwave (SW) and longwave (LW) radiation, sensible heat (SH) and latent heat (LH) fluxes, plus the heat flux into the ground (G, including a small contribution due to snowmelt). In Eq. (2), LW, SH, and LH are positive upward whereas SW and G are positive downward. Atmospheric transports

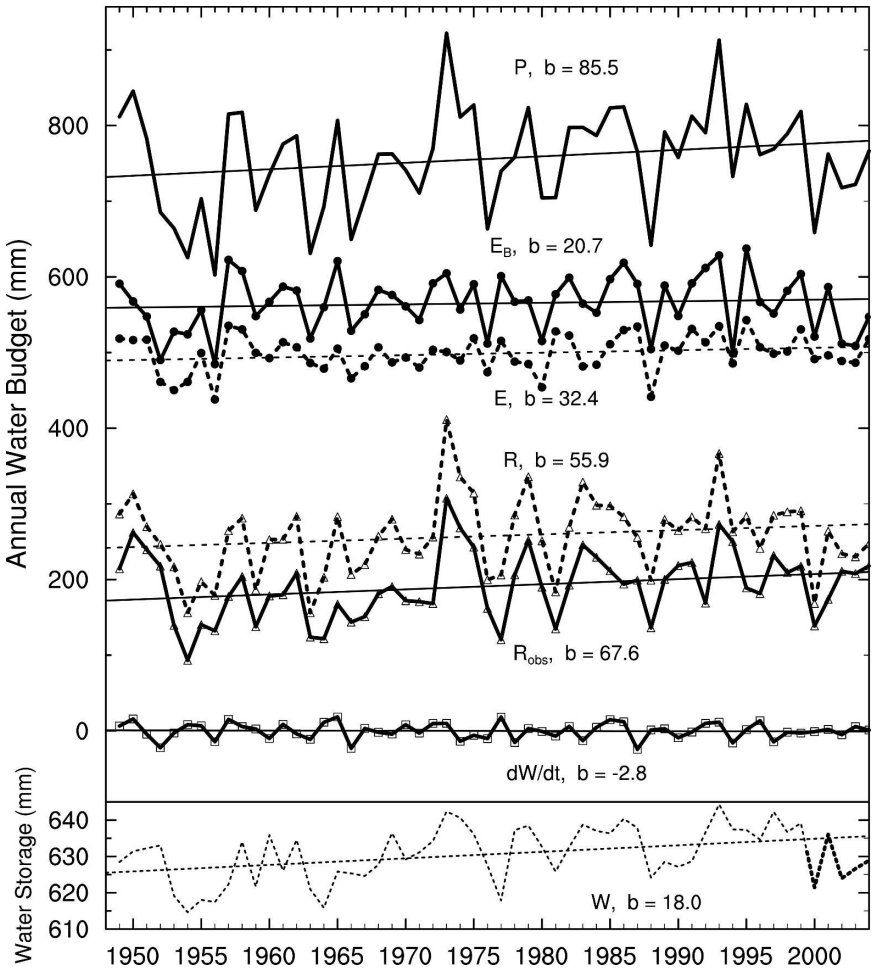

FIG. 1. Time series of annual (water year) surface water budget components averaged over the Mississippi River basin and associated linear trends (straight lines: b is the slope in mm century^{-1}). Given are the observed basin precipitation (P, solid line), runoff (R_{obs}, solid line with triangles), the water budget-derived evapotranspiration (E_B, solid line with dots), and CLM3-simulated runoff (R, dashed line with triangles), evapotranspiration (E, dashed line with dots), change of land water storage [dW/dt, solid line with quadrangles; note that b for this quantity is $d(dW/dt)/dt$] and (bottom) land water storage (W, dashed line; b is the trend in W).

may affect these quantities by altering surface air temperature and humidity. Except for downward shortwave (SW↓), which is derived from observed cloud cover, all other energy budget components are from the observation-constrained CLM3 simulation. Trends in all time series data are analyzed using simple linear regression.

3. Results

a. Surface water budget

Figure 1 shows the time series of the annual mean of the terms in Eq. (1) based on either observations or the observation-constrained CLM3 simulations for the Mississippi basin, with the linear trends summarized in Table 1. From October 1948 to September 2004, the basin-averaged precipitation (solid line) increased at an average rate of 85.5 ± 7.4 mm century^{-1} or ~11.3 ± 1.0% century^{-1} (attained significance level $p = 0.13$). The observed runoff (solid line with triangles) has similarly increased at a rate of 67.6 ± 4.8 mm century^{-1} or ~35.3 ± 2.5% century^{-1} ($p = 0.07$). The precipitation and runoff trends are compared with previous studies in Table 2. Karl and Knight (1998) reported a U.S. annual mean precipitation increase of 65–151 mm century^{-1}, or 7.7%–19.5% century^{-1}, for different periods and different datasets. Groisman et al. (2004) updated U.S.

TABLE 1. Annual (water year) trends from October 1948 to September 2004 of the water budget components averaged over the Mississippi basin as shown in Fig. 1.

Variables	Basin mean (mm)	Slope b (mm century^{-1})	Standard error of b (mm century^{-1})	p value	Correlation
Precipitation	756	85.5	7.4	0.13	
Runoff	258	55.9	5.6	0.19	0.90 (vs R_{obs})
Evapotrannspiration	499	32.4	2.7	0.11	0.82 (vs E_B)
dW/dt	0	−2.8	1.2	0.75	
R_{obs}	191	67.6	4.8	0.07	
E_B	565	20.7	4.2	0.51	

annual precipitation trends for 1908–2002 and annual runoff trends for 1939–2002, and found them to be 7% and 26% century^{-1}, respectively. For the Mississippi basin, Walter et al. (2004) estimated increases of annual precipitation of 176 mm century^{-1} and for streamflow of 65 mm century^{-1} from 1950 to 2000. Although these linear trends differ somewhat, they are all for slightly different time periods, and our precipitation and streamflow trends are generally consistent with them.

Substantial biases in rain gauge records of precipitation exist because of undercatch (especially for snow) due to winds and evaporation within the gauge. Yang et al. (2005) adjusted daily precipitation records from 4802 high-latitude stations to correct for the biases of wind-induced undercatch, wetting losses, and trace precipitation amounts for the last 30 yr. Bias corrections generally enhance monthly precipitation trends by 5%–20%. In this study the precipitation data were not corrected for undercatch and other biases over the United States. The observed streamflow is affected by human withdrawals and water management. Although water resource development has played only a small role in the time-mean water balance, Milly and Dunne (2001) estimated that irrigation and other human activities (consumptive water use) may have contributed about 26 mm century^{-1} (or >25%) to the increasing trend in total evaporation over the Mississippi basin, while the storage rates associated with filling of surface reservoirs and long-term depletion of groundwater were estimated as 5 and 3 mm century^{-1}, respectively. Gedney et al. (2006) recently suggested that the increasing runoff trends are consistent with a suppression of plant transpiration due to CO_2-induced stomatal closure.

The CLM3-simulated runoff (Fig. 1, dashed line with triangles) increased at a rate of 55.9 ± 5.6 mm century^{-1}, or about 21.7 ± 2.2% century^{-1} (relative to the simulated mean, $p = 0.19$). It is highly correlated with the observed annual runoff ($r = 0.90$, with mean bias of 66.3 mm or 34.6% of the observed mean). The CLM3-simulated evapotranspiration (dashed line with dots) increased at a rate of 32.4 ± 2.7 mm century^{-1}, or about 6.5 ± 0.5% century^{-1} ($p = 0.11$). Although the CLM3-simulated land water storage W (Fig. 1, bottom) increased at a rate of 18.0 mm century^{-1} ($p < 0.01$), the trend in the change of water storage [dW/dt, its trend is $d(dW/dt)/dt$], which is dominated by changes in soil water, decreased at a very small and insignificant rate of 2.8 mm century^{-1}. The water budget–derived evapo-

TABLE 2. Annual precipitation and runoff trends from different datasets and different periods.

Studies	Region	Period of precipitation	Precipitation trend (mm century^{-1})/(% century^{-1})	Period of runoff	Runoff trend (mm century^{-1})/(% century^{-1})
Karl and Knight (1998)					
HCNs	United States	1910–96	81/10.1		
CD	United States	1910–96	76/10.0		
CD	United States	1910–96	65/7.7		
TD 3200	United States	1948–95	128/16.9		
HCNs	United States	1948–95	110/14.7		
CD	United States	1948–95	151/19.5		
Groisman et al. (2004)	United States	1908–2002	53/7	1939–2002	N/A/26
Walter et al. (2004)	Mississippi	1950–2000	176/N/A	1950–2000	65/N/A
Present study	Mississippi	1948–2004	85.5/11	1948–2004	68/35
	Mississippi	1950–2000	171/23	1950–2000	81/31

HCNs: Historical Climate Network special network.
CD: the U.S. climatological division dataset.

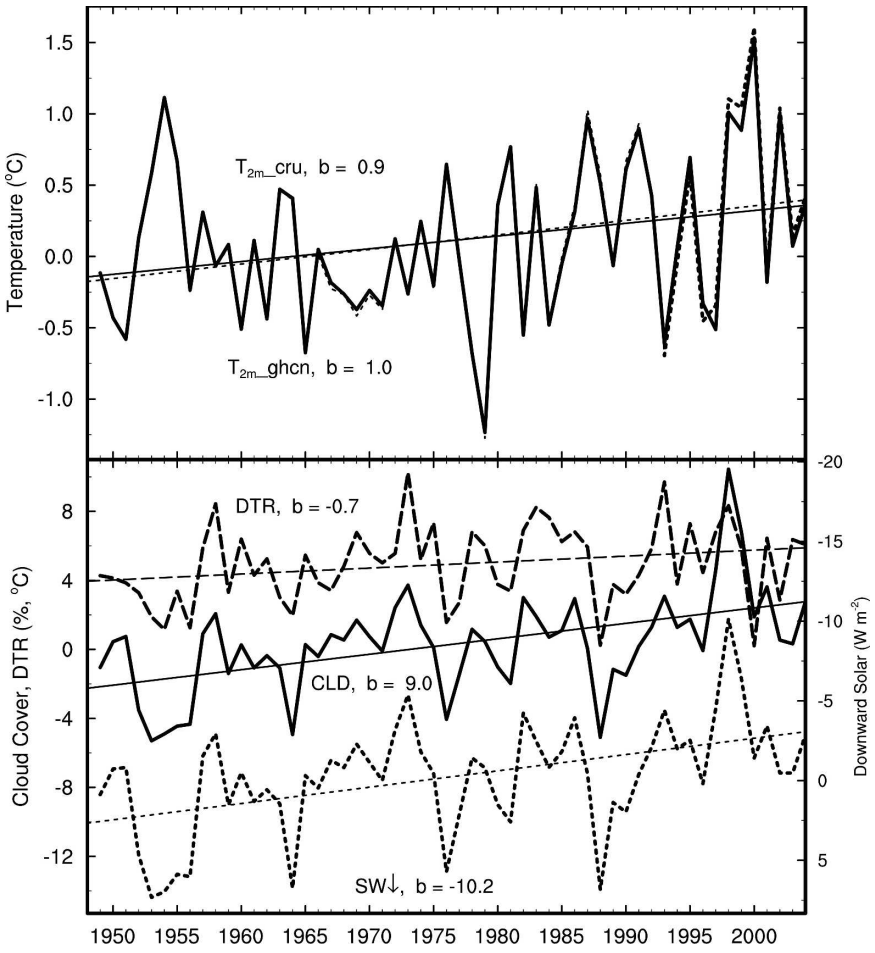

FIG. 2. Anomaly time series of observed annual (water year) (top) surface air temperature from the CRU dataset (T_{2m}_cru, solid line) and the GHCN2 dataset (T_{2m}_ghcn, short dashed line), and (bottom) cloud cover (CLD, solid line), and diurnal temperature range [DTR, long dashed line; scaled as –5DTR+5, from Dai et al. (2006)], and cloud-adjusted downward solar radiation ($SW\downarrow$, short dashed line; increases downward on the right ordinate) in the averaged over the Mississippi River basin and associated linear trends (straight lines: b is the slope, °C century^{-1} for T and DTR, % century^{-1} for CLD, and W m^{-2} century^{-1} for SW↓).

transpiration (E_B, where B is budget; solid line with dots), as the residual of precipitation, observed runoff, and CLM3-simulated change of water storage, also increased at a rate of 20.7 ± 4.2 mm century^{-1}, or about 3.7 ± 0.7% century^{-1} (p = 0.51). It is correlated with the model-simulated evapotranspiration (r = 0.82), which has a larger increase of 32.4 mm century^{-1}. Therefore, in terms of linear trends, the increase of precipitation is compensated by both runoff (65%) and evapotranspiration (38%, based on E_B), plus a small loss of change of water storage (as shown schematically later in Fig. 6). The increasing trend is consistent with the results of previous mass balance studies (Milly and Dunne 2001; Walter et al. 2004). As the contribution from change of water storage is about 3%, this study actually adds credence to earlier mass balance approaches in which they assumed that internal net water storage is negligible.

b. *Temperature, cloud, and diurnal temperature range*

The Mississippi River basin-averaged temperature from the CRU dataset increased linearly at a rate of 0.9° ± 0.1°C century^{-1} (p = 0.05) from 1948 to 2004 (Fig. 2, top, solid line, Table 3). The temperature from the GHCN2 homogeneity-adjusted data (dashed line) also increased, at a similar rate of 1.0° ± 0.1°C century^{-1} (p = 0.03). These values agree within the standard error of slope b (Table 3). Linear trends are quite

TABLE 3. Annual (water year) trends from October 1948 to September 2004 of 2-m air temperature, total cloud cover, DTR, and downward shortwave radiation averaged over the Mississippi Basin, as shown in Fig. 2.

Variables	Basin mean	Slope b	Standard error of b	b units	p value	Correlation
T_{2m}_ghcn	11.0 (°C)	1.0	0.1	(°C century^{-1})	0.03	
T_{2m}_cru	10.2 (°C)	0.9	0.1	(°C century^{-1})	0.05	
Cloud		9.0	0.3	(% century^{-1})	<0.01	0.62 (vs P)
DTR		−0.7	0.1	(°C century^{-1})	0.06	−0.72 (vs cloud)
SW↓	178 (Wm^{-2})	10.2	0.3	(W m^{-2} century^{-1})	<0.01	

a lot less (0.3°C century^{-1}) for 1949–1997, which was the period analyzed by Milly and Dunne (2001) using the original uncorrected station data (P. C. D. Milly 2006, personal communications), but station temperature data from many U.S. stations contain large nonclimatic changes due to instrumental changes (Peterson and Vose 1997), and the adjustments in GHCN2 remove most of these nonclimatic changes. Thus the homogeneity-adjusted GHCN2 data used here are likely more reliable than Milly and Dunne (2001).

The DTR from the GHCN2 shows an overall linear decreasing trend of 0.7 ± 0.1°C century^{-1} ($p = 0.06$) from 1948 to 2004 over the Mississippi River basin (Fig. 2, bottom, long dashed line, scaled as –5DTR+5). The DTR decreases, together with the upward trend in precipitation (Fig. 1), are physically consistent with the increasing trend of 9.0 ± 0.3% century^{-1} of sky ($p < 0.01$) in observed total cloud cover from 1948 to 2004 (solid line), as clouds have a dominant damping effect on the DTR (Dai et al. 1999). Correspondingly, the cloud-adjusted downward solar radiation (short dashed line, right-hand ordinate) decreased at a rate of 10.2 ± 0.3 W m^{-2} century^{-1} ($p < 0.01$). Increasing anthropogenic aerosol concentrations (Stanhill and Cohen 2001), the extinction effects of volcanic eruptions (Schwartz 2005), or the population/urbanization effect (Alpert et al. 2005) may contribute to solar dimming in some locations. Whether the increased cloud cover is due to these factors cannot, however, be ascertained.

c. Surface energy budget

Figure 3 shows the 1948–2004 time series of the annual anomalies for the surface energy budget components. The downward shortwave flux SW↓ (thick solid line with dots) decreased by 10.2 ± 0.3 W m^{-2} century^{-1}, and the reflected upward shortwave flux SW↑ (thick dashed line with triangles) decreased by 4.6 ± 0.1 W m^{-2} century^{-1}. This implies that the net shortwave flux F_{sw} (positive downward) decreased by 5.7 ± 0.3 W m^{-2} century^{-1}, or about 4.3 ± 0.2% century^{-1} ($p = 0.01$; Table 4).

Figure 3 shows that the downward longwave flux LW↓ (thin solid line with dots) increased by 11.6 ± 0.3 W m^{-2} century^{-1}, and the emitted upward longwave flux LW↑ (thin dashed line with triangles) increased by 5.3 ± 0.3 W m^{-2} century^{-1}. This implies that the net longwave flux F_{lw} (positive upward) decreased, at a rate of 6.3 ± 0.2 W m^{-2} century^{-1}, or 9.9 ± 0.3% century^{-1} ($p < 0.01$). Therefore, the atmospheric longwave radiation increases have largely offset solar radiation decreases. This corroborates the earlier hypothesis by Walter et al. (2004).

Although both ground and air temperatures increased from 1948 to 2004, the increasing rate for ground temperature is less than that for surface air temperature (not shown). These are consistent with the changes in net longwave radiation in which LW↓ increased by 11.6 W m^{-2} century^{-1} while LW↑ increased by only 5.3 W m^{-2} century^{-1}. Also, as a result, the surface sensible heat flux decreased by 1.8 ± 0.3 W m^{-2}, or 6.5 ± 1.1% century^{-1} ($p = 0.43$) (Fig. 3, long dashed line), while the latent heat flux (short dashed line) increased at a rate of 2.5 ± 0.2 W m^{-2}, or about 6.3 ± 0.5% century^{-1} ($p = 0.12$). Note that sensible and latent heat fluxes vary inversely ($r = -0.63$), as expected from the repartitioning of energy with changes in surface moisture (LeMone et al. 2003; Trenberth and Shea 2005).

The residual (heat flux into soil, bottom line in Fig. 3) is very small. Therefore, in terms of long-term changes, there are strong compensations between net shortwave and longwave radiation ($r = 0.65$) and between sensible and latent heat fluxes ($r = -0.63$). Hence the change in net total radiation is small. Overall, the decreases in net longwave radiation and sensible heat flux not only offset the reduction in shortwave radiation but also allow an increase in latent heat flux. This is depicted schematically in Fig. 6, described later. Therefore, the surface heat balance is a four-way balance, and the increase of latent heat flux is not caused by the change of

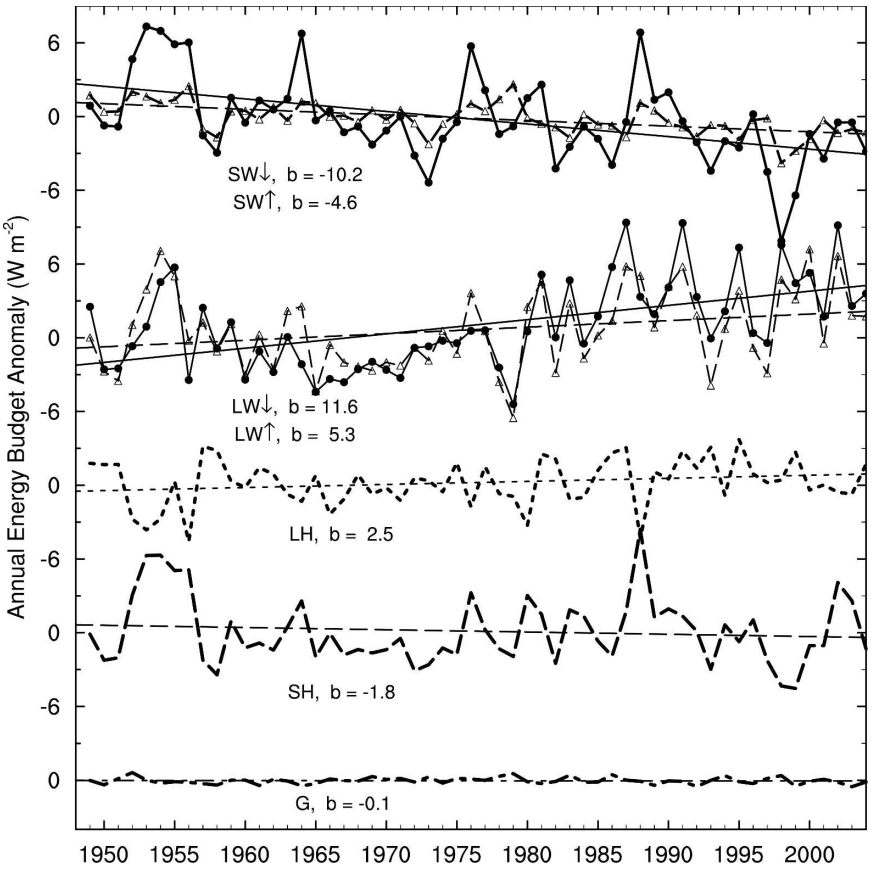

FIG. 3. Annual (water year) anomaly time series of surface energy budget components averaged over the Mississippi River basin and associated linear trends (straight lines: b is the slope, in W m^{-2} century^{-1}). Except for downward shortwave (SW↓, thick solid line with dots), which is derived from observed cloud cover, all other components are from the observation-constrained CLM3 simulation: upward shortwave (SW↑, thick dashed line with triangles), downward longwave (LW↓, thin solid line with dots), upward longwave (LW↑, thin dashed line with triangles), latent heat flux (LH, short dashed line), sensible heat flux (SH, long dashed line), and heat flux into the ground (G, bottom line).

shortwave flux. This does not support the assumed two-way balance between latent heat flux and shortwave flux in Roderick and Farquhar (2002) or the incomplete balance in Wild et al. (2004).

d. Sensitivity experiments on factors affecting evapotranspiration trends

While isolating one factor and fixing other factors is idealistic, it can be useful to see how linear the different factors are. For example, increases in precipitation are usually associated with decreases in air temperature and increases in cloud amount, and increases of cloud amount are associated with decreases of downward shortwave radiation and increases of downward longwave radiation. However, such idealized experiments do help us understand the dominant factors affecting the final evapotranspiration trend.

Figure 4 shows the results from sensitivity experiments that explore factors affecting the evapotranspiration trend. The solid line is from the standard run (same as the dashed line with dots in Fig. 1). The short dashed line is from a run forced with varying precipitation but fixed other forcing [i.e., other forcings were set to the data of a specific year (1979) for 1948–2004; dP run]. The resultant E trend is 55.6 mm century^{-1} ($p = 0.05$), larger than the trend of 32.4 mm century^{-1} ($p = 0.11$) in the standard (all forcing) run. The long dashed line is from a run with only temperature forcing (others fixed, dT run). The trend in this run is 3.6 mm century^{-1} ($p = 0.45$), much smaller than that in the standard run. The bottom line in Fig. 4 is from a run with only downward solar radiation (i.e., cloud) forcing (dSW↓ run), and it has a negative trend of −23.5 mm per century ($p < 0.01$). This is expected, as decreasing

TABLE 4. Annual (water year) trends from October 1948 to September 2004 of the energy budget components averaged over the Mississippi Basin, as shown in Fig. 3.

Variables	Basin mean ($W\ m^{-2}$)	Slope b ($W\ m^{-2}\ century^{-1}$)	Standard error of b ($W\ m^{-2}\ century^{-1}$)	p value	Correlation
SW↓	178	−10.2	0.3	<0.01	
SW↑	47	−4.6	0.1	<0.01	
F_{sw}	131	−5.7	0.3	0.01	
LW↓	309	11.6	0.3	<0.01	
LW↑	372	5.3	0.3	0.04	
F_{lw}	63	−6.3	0.2	<0.01	0.65 (vs F_{sw})
LH	40	2.5	0.2	0.12	
SH	28	−1.8	0.3	0.43	−0.63 (vs LH)
G	1	−0.1	0.0	0.82	

solar radiation reduces surface energy available for evapotranspiration if there are no other changes. In addition, we have calculated the correlation between the simulated evapotranspiration and the forcing variables. The correlation with precipitation is 0.72, with temperature is −0.01, and with downward shortwave radiation is −0.53. Therefore, these results suggest that the increase in evapotranspiration from 1948 to 2004

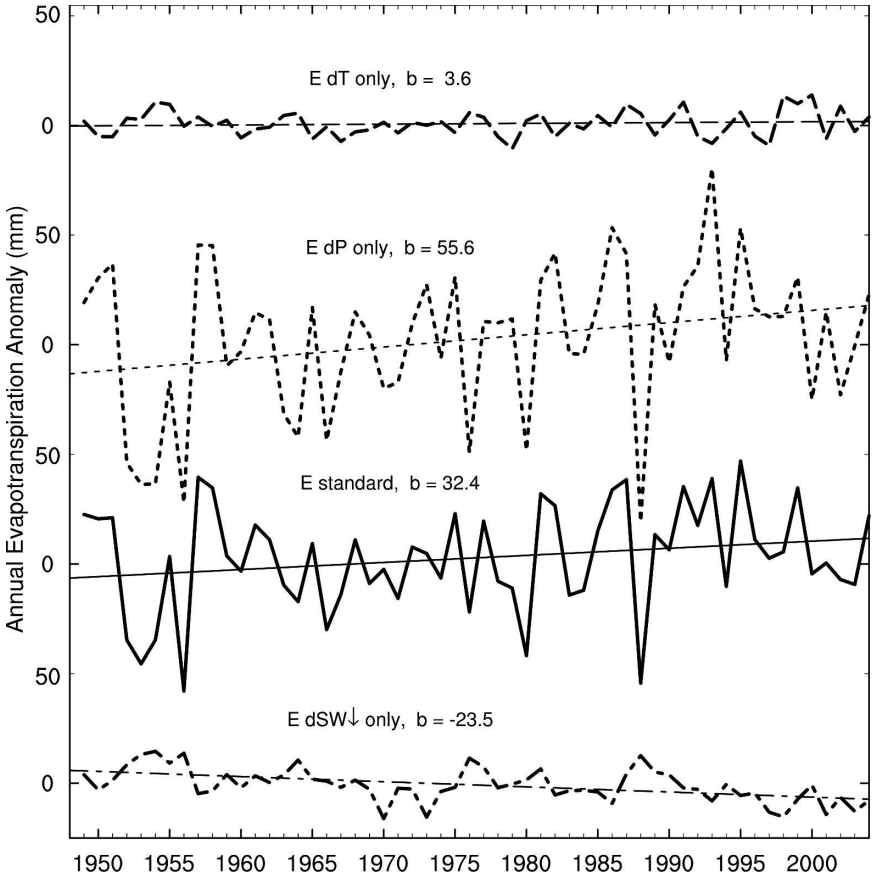

FIG. 4. Anomaly time series of annual (water year) surface evapotranspiration averaged over the Mississippi River basin and associated linear trends (straight line: b is the slope, in mm $century^{-1}$) from CLM3 sensitivity experiments: Standard = all forcing run (solid line); dP only = with only precipitation changing and other forcings fixed (short dashed line); dT only = run with only temperature changing (long dashed line); dSW↓ only = with only downward solar radiation (i.e., cloud) changing (bottom line).

was induced predominantly by the increase in precipitation, and partly offset by cloud-induced reduction in solar radiation.

e. Spatial distributions of trends

Figures 5a–d show the linear trend maps of the water budget terms over the contiguous United States. The stippled area is the Mississippi River basin with the dark line as the boundary. Precipitation (Fig. 5a) increased over the entire basin during 1948–2004 with the largest increases in the central part of the basin. Over the central and eastern part of the basin, CLM3-simulated runoff (Fig. 5b) increased while trends in evapotranspiration (Fig. 5c) are relatively small. Over the western part of the basin, evapotranspiration increased while trends in runoff are small. Trends in change of land water storage are very small over most of the basin (Fig. 5d).

The trend pattern in evapotranspiration is determined by several factors. Over the western part of the basin, surface soil and air are relatively dry (Dai 2006), runoff is limited, and water is a limiting factor for evapotranspiration, whereas atmospheric demand, as given through temperature and energy supply, is important over the relatively wet central and eastern part of the basin. Consequently, trends in evapotranspiration in the western part follow more closely the precipitation changes even though cloud-inferred downward solar radiation decreased (Figs. 5f–g), whereas decreasing solar radiation over the eastern part largely offsets the positive impact of increasing precipitation on evapotranspiration.

Surface air temperature (Fig. 5e) shows large increases (0.8°–2.4°C century^{-1}) during 1948–2004 in the northern and western part of the Mississippi basin, while little change or small cooling is seen in the southeast of the basin, consistent with the results of Groisman et al. (2004). Total cloud cover (Fig. 5f) increased over most of the basin by about 4%–12% of sky century^{-1} and is the main cause for the reduced surface net shortwave radiation shown in Fig. 5g.

The trend maps of the energy budget terms during 1948–2004 (Figs. 5g–j) show that the decreasing trend pattern in net shortwave radiation (Fig. 5g) (by about 2–12 W m^{-2} century^{-1} over the Mississippi basin) generally follows the cloudiness change map (Fig. 5f). The net longwave flux (Fig. 5i) decreased by 4–12 W m^{-2} century^{-1} over most of the Mississippi basin, although the trend in the western half is about twice as large as in the eastern half. Surface latent heat flux (Fig. 5h), which is essentially surface evapotranspiration (Fig. 5c), increased (by 2–12 W m^{-2} century^{-1}) over the central and western United States, but decreased (by 2–4 W m^{-2} century^{-1}) in the eastern part of the country. Surface sensible heat flux (Fig. 5j) increased (by 2–8 W m^{-2} century^{-1}) in the northwestern part of the basin, but decreased (by 2–8 W m^{-2} century^{-1}) in the other parts of the basin. Therefore, the strong compensation between short- and longwave radiation occurs on regional and local scales (Fig. 5k). The net radiation increased (by 2–6 W m^{-2} century^{-1}) in the western part of the basin, but decreased (by 2–6 W m^{-2} century^{-1}) in the eastern part of the basin. Similarly, there is strong compensation between sensible and latent heat fluxes on regional and local scales (Fig. 5l). Thus, the large decrease in the net longwave radiation (positive upward) not only offsets the reduced solar radiation but further provides energy for enhanced evapotranspiration (i.e., increased LH flux) over the western and eastern United States; whereas in the eastern part, reduced SH flux also contributes to balance the decrease in solar radiation. Over the Mississippi basin, sensible heat flux also plays an important role in balancing the surface energy budget.

4. Summary and discussion

Changes in the surface water and energy budget components over the Mississippi River basin during 1948–2004 have been investigated using a combination of hydroclimatic records and observation-constrained simulations of the land surface conditions using a comprehensive land surface model (namely, the CLM3). The atmospheric forcing for driving the CLM3 were constructed by combining observed monthly precipitation, temperature, and cloud cover with intramonthly variations derived from the 6-hourly NCEP–NCAR reanalysis.

In the offline observation-constrained CLM3 runs, the atmospheric downward longwave radiation is derived from the surface air temperature and vapor pressure without considering clouds. Since lower-tropospheric air temperature and water vapor control downward longwave radiation at the surface with only small effects from clouds outside the polar regions (Zhang et al. 1995), the longwave fluxes from the CLM3 simulations may be considered as a first-order estimate. We did not use the NCEP–NCAR reanalysis downward longwave radiation because its air temperature and cloud trends are problematic. Although the NARR surface air temperature trend over the Mississippi Basin is quite consistent with the observation, the total cloud cover shows a decreasing trend of -4.8% century^{-1} from 1979 to 2004, which is opposite to the increasing trend from observation (16.6% century^{-1}). Reliable records of surface longwave radiation measurements are generally

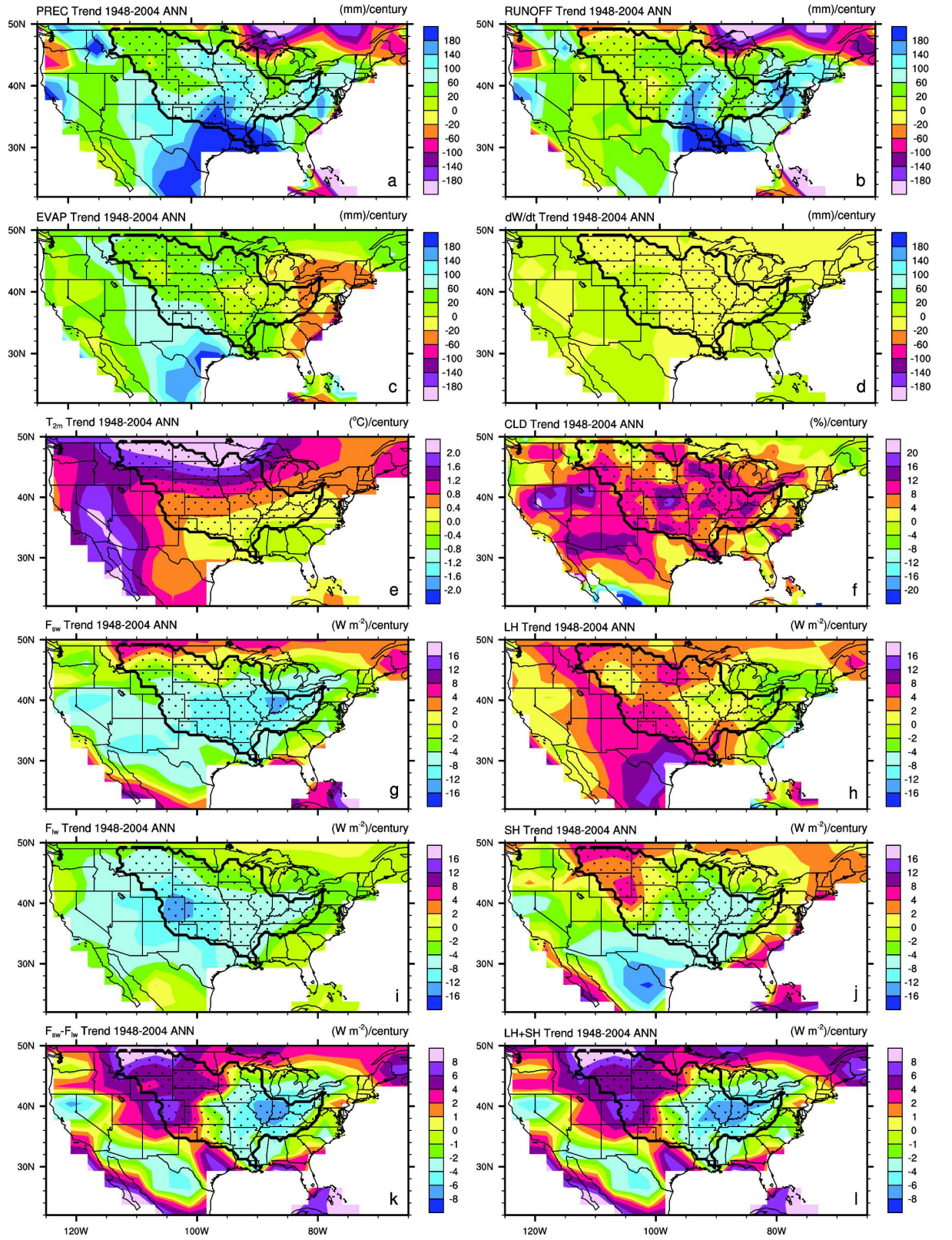

FIG. 5. Spatial distributions of the linear trend from October 1948 to September 2004 in annual (water year) (a) observed precipitation; CLM3-simulated (b) runoff, (c) evapotranspiration, and (d) change of water storage; (e) observed surface air temperature; (f) observed cloud amount; and CLM3-simulated (g) net shortwave radiation, (h) latent heat flux, (i) net longwave radiation, (j) sensible heat flux, (k) net radiative heating, and (l) net turbulent flux. The stippled area is the Mississippi basin with the dark line as the boundary.

unavailable prior to the 1990s. Philipona et al. (2004) found a significant increase in downward longwave radiation observed at several stations in the Swiss Alps between 1995 and 2002. As clouds affect surface downward longwave radiation by changing atmospheric emissivity, Crawford and Duchon (1999) showed that increasing clouds imply increased downward surface longwave radiation. We infer that, if clouds had been included in the offline CLM3 downward longwave radiation calculation, the net longwave flux would be decreasing at a larger rate, which would further mitigate the effect of reduced solar radiation on evapotranspiration. Philipona and Dürr (2004) showed that increases in surface net radiative heating over central Europe for the periods 1995–2003 were dominated by the clear-sky longwave radiation component resulting from an enhanced water vapor greenhouse effect, while the effects of changing cloud amounts on downward solar radiation and downward longwave radiation compensated each other and had little effect on annual-mean surface warming.

To a surprising extent, the main changes in both water and energy budget components for 1948 to 2004 can be characterized by linear trends that seem to be physical (real, not bad data) and statistically significant, and the trends in different variables are physically consistent with one another. This justifies our focus on linear trends, part of which is a posteriori reasoning.

The results of basin-averaged linear trends in water and energy budgets during 1948–2004 are summarized schematically in Fig. 6 in which the downward arrow means that the flux increases the trend of *dW/dt* or *G*. For the surface water budget, the increase in observed basin-averaged precipitation (85.5 mm century^{-1}) is compensated by the increases in both observed runoff (67.5 mm century^{-1}) and inferred evapotranspiration (20.7 mm century^{-1}), with only a small decrease in the change of land water storage (2.8 mm century^{-1}). For the surface energy budget, the decrease of net solar radiation (5.7 W m^{-2} century^{-1}) associated with the observed increase in cloud cover (9.0% sky century^{-1}) is compensated by a decrease of net longwave radiation (6.3 W m^{-2} century^{-1}) and sensible heat flux (1.8 W m^{-2} century^{-1}), while the latent heat flux increases (by 2.5 W m^{-2} century^{-1}) in association with increased precipitation and enhanced longwave radiative heating. Our results of both the surface water and energy budgets support the notion that evapotranspiration has increased over the Mississippi River basin during 1948–2004, although the basin-averaged evapotranspiration and latent heat flux trends are not statistically significant. Sensitivity experiments suggest that the evapotranspiration trend mainly results from the precipitation change, with smaller effects from the temperature and solar radiation changes.

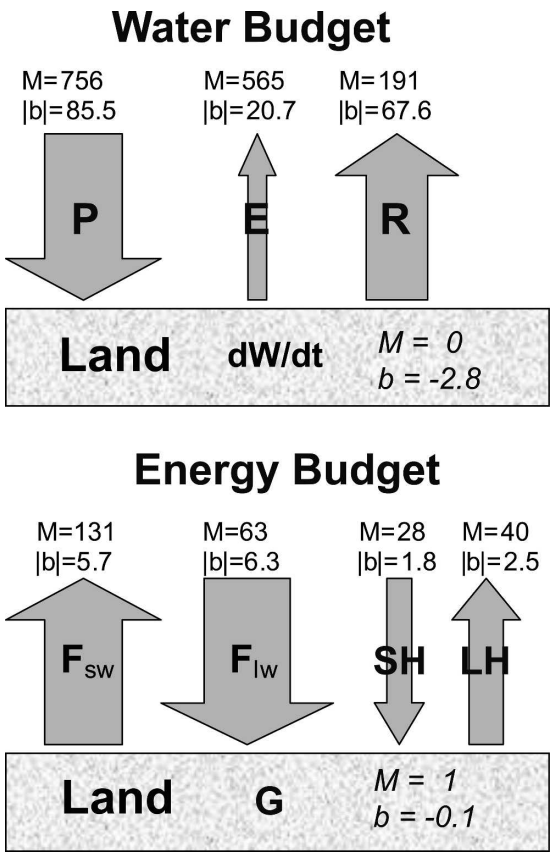

FIG. 6. Basin-averaged trends in the water and energy budget components for the Mississippi River basin: *M* is the long-term (1948–2004) annual (water year) mean (in mm for water components and W m^{-2} for energy components) and *b* is the annual linear trend during 1948–2004 (in mm century^{-1} for water components and W m^{-2} century^{-1} for energy components, proportional to arrow shaft width). Note that the downward arrow means that the flux increases the trend of *dW/dt* or *G*.

Our results also show that the change in surface sensible heat flux is comparable with changes in the other energy components. Thus it should be included in the energy budget analysis, although it has often been ignored (Wild et al. 2004). The surface net radiative heating (F_{sw}–F_{lw}, positive downward) increased by 0.6 W m^{-2} century^{-1}, which is only one-third of the change in sensible heat flux (1.8 W m^{-2} century^{-1}). As mentioned in the introduction, many previous studies considered only the change in downward solar radiation (i.e., dimming), which is insufficient for assessing the change in the energy budget.

However, it is evident that changes are not uniform across the basin. Observed precipitation increases in the central and eastern parts of the Mississippi basin are balanced mainly by increased runoff, with small

changes in evapotranspiration; while over the western part of the basin increased precipitation results in enhanced evapotranspiration but little change in runoff. The decrease of the net shortwave radiation is mainly compensated by the reduction in upward net longwave radiation in the western part of the basin, but also with contributions from reduced sensible heat flux in the eastern part of the basin. The spatial patterns of the trends are consistent with the fact that in water-limited environments (such as the arid western United States) surface evapotranspiration is mainly controlled by available water (Hobbins et al. 2004), whereas over the relatively wet central and eastern United States, available energy plays an important role in regulating surface evapotranspiration.

This study also has several limitations, including uncertainties in model forcing data and deficiencies in the CLM3. The uncertainties in the forcing data include undercatch and topography-induced biases in precipitation, the adjustment of the solar radiation using the often incomplete cloudiness data, and a lack of realistic accounting of LW–cloud interaction. The CLM3 may have been tuned to unrealistic high frequency and low intensity of precipitation (Dai and Trenberth 2004), and it needs improved representations of land hydrology such as the partitioning of evapotranspiration (Wu and Dickinson 2005; Dickinson et al. 2006), as well as treatment of human influences on natural streamflow and groundwater. Currently a bunch of improvements are ongoing, for example, on the partitioning of evapotranspiration (Lawrence et al. 2007), soil water availability, and soil evaporation (K. W. Oleson et al. 2007, personal communication), surface and subsurface runoff (Niu et al. 2005), and groundwater and water table depth (Niu et al. 2007). Future improvements in these aspects are expected to decrease the uncertainties in the estimated hydroclimatic trends.

Acknowledgments. This work was supported by NSF Grant ATM-0233568 and NCAR TIIMES Water Cycles across Scales Project. The first author would like to thank Dennis Shea and Adam Phillips for their help with the NCL scripts. We also thank Andy Pitman and three anonymous reviewers for their thorough and perceptive reviews that did much to improve the manuscript.

REFERENCES

Adler, R. F., and Coauthors, 2003: The Version-2 Global Precipitation Climatology Project (GPCP) monthly precipitation analysis (1979–present). *J. Hydrometeor.,* **4,** 1147–1167.

Alpert, P., P. Kishcha, Y. J. Kaufman, and R. Schwarzbard, 2005: Global dimming or local dimming?: Effect of urbanization on sunlight availability. *Geophys. Res. Lett.,* **32,** L17802, doi:10.1029/2005GL023320.

Baldocchi, D., and Coauthors, 2001: FLUXNET: A new tool to study the temporal and spatial variability of ecosystem-scale carbon dioxide, water vapor, and energy flux densities. *Bull. Amer. Meteor. Soc.,* **82,** 2415–2434.

Brutsaert, W., and M. B. Parlange, 1998: Hydrologic cycle explains the evaporation paradox. *Nature,* **396,** 29–30.

Chattopadhyay, N., and M. Hulme, 1997: Evaporation and potential evapotranspiration in India under conditions of recent and future climate change. *Agric. For. Meteor.,* **87,** 55–73.

Chen, M., P. Xie, J. E. Janowiak, and P. A. Arkin, 2002: Global land precipitation: A 50-yr monthly analysis based on gauge observations. *J. Hydrometeor.,* **3,** 249–266.

Crawford, T. M., and C. E. Duchon, 1999: An improved parameterization for estimating effective atmospheric emissivity for use in calculating daytime downwelling longwave radiation. *J. Appl. Meteor.,* **38,** 474–480.

Dai, A., 2006: Recent climatology, variability, and trends in global surface humidity. *J. Climate,* **19,** 3589–3606.

——, and K. E. Trenberth, 2002: Estimates of freshwater discharge from continents: Latitudinal and seasonal variations. *J. Hydrometeor.,* **3,** 660–687.

——, and ——, 2004: The diurnal cycle and its depiction in the Community Climate System Model. *J. Climate,* **17,** 930–951.

——, A. D. Del Genio, and I. Y. Fung, 1997a: Clouds, precipitation, and temperature range. *Nature,* **386,** 665–666.

——, I. Y. Fung, and A. D. Del Genio, 1997b: Surface observed global land precipitation variations during 1900–88. *J. Climate,* **10,** 2943–2962.

——, K. E. Trenberth, and T. R. Karl, 1999: Effects of clouds, soil moisture, precipitation, and water vapor on diurnal temperature range. *J. Climate,* **12,** 2451–2473.

——, T. R. Karl, B. Sun, and K. E. Trenberth, 2006: Recent trends in cloudiness over the United States: A tale of monitoring inadequacies. *Bull. Amer. Meteor. Soc.,* **87,** 597–606.

Dai, Y., and Coauthors, 2003: The Common Land Model. *Bull. Amer. Meteor. Soc.,* **84,** 1013–1023.

Dickinson, R. E., K. W. Oleson, G. B. Bonan, F. Hoffman, P. Thornton, M. Vertenstein, Z.-L. Yang, and X. Zeng, 2006: The Community Land Model and its climate statistics as a component of the Community Climate System Model. *J. Climate,* **19,** 2302–2324.

Dirmeyer, P. A., A. J. Dolman, and N. Sato, 1999: The pilot phase of the Global Soil Wetness Project. *Bull. Amer. Meteor. Soc.,* **80,** 851–878.

Easterling, D. R., and Coauthors, 1997: Maximum and minimum temperature trends for the globe. *Science,* **277,** 364–367.

Fan, Y., H. M. Van den Dool, D. Lohmann, and K. Mitchell, 2006: 1948–98 U.S. hydrological reanalysis by the Noah land data assimilation system. *J. Climate,* **19,** 1214–1237.

Gedney, N., P. M. Cox, R. A. Betts, O. Boucher, C. Huntingford, and P. A. Stott, 2006: Detection of a direct carbon dioxide effect in continental river runoff records. *Nature,* **439,** 835–838.

Gilgen, H., M. Wild, and A. Ohmura, 1998: Means and trends of shortwave irradiance at the surface estimated from Global Energy Balance Archive data. *J. Climate,* **11,** 2042–2061.

Golubev, V. S., J. H. Lawrimore, P. Ya. Groisman, N. A. Speranskaya, S. A. Zhuravin, M. J. Menne, T. C. Peterson, and R. W. Malone, 2001: Evaporation changes over the contiguous United States and the former USSR: A reassessment. *Geophys. Res. Lett.,* **28,** 2665–2668.

Groisman, P. Ya., and Coauthors, 1999: Changes in the probability of heavy precipitation: Important indicators of climatic change. *Climatic Change,* **42,** 243–283.

——, R. W. Knight, and T. R. Karl, 2001: Heavy precipitation and high streamflow in the contiguous United States: Trends in the twentieth century. *Bull. Amer. Meteor. Soc.,* **82,** 219–246.

——, ——, ——, D. R. Easterling, B. Sun, and J. H. Lawrimore, 2004: Contemporary changes of the hydrological cycle over the contiguous United States: Trends derived from in situ observations. *J. Hydrometeor.,* **5,** 64–85.

Hobbins, M. T., J. A. Ramirez, and T. C. Brown, 2004: Trends in pan evaporation and actual evapotranspiration across the conterminous U.S.: Paradoxical or complementary? *Geophys. Res. Lett.,* **31,** L13503, doi:10.1029/2004GL019846.

Houghton, J. T., Y. Ding, D. C. Griggs, M. Noguer, P. J. van der Linden, X. Dai, K. Maskell, and C. A. Johnson, Eds., 2001: *Climate Change 2001: The Scientific Basis*. Cambridge University Press, 881 pp.

Huntington, T. G., 2006: Evidence for intensification of the global water cycle: Review and synthesis. *J. Hydrol.,* **319,** 83–95.

Jones, P. D., and A. Moberg, 2003: Hemispheric and large-scale surface air temperature variations: An extensive revision and an update to 2001. *J. Climate,* **16,** 206–223.

Kalnay, E., and Coauthors, 1996: The NCEP/NCAR 40-Year Reanalysis Project. *Bull. Amer. Meteor. Soc.,* **77,** 437–471.

Karl, T. R., and P. M. Steurer, 1990: Increased cloudiness in the United States during the first half of the twentieth century: Fact or fiction? *Geophys. Res. Lett.,* **17,** 1925–1928.

——, and R. W. Knight, 1998: Secular trends of precipitation amount, frequency, and intensity in the United States. *Bull. Amer. Meteor. Soc.,* **79,** 231–241.

Koster, R. D., and Coauthors, 2004: Regions of strong coupling between soil moisture and precipitation. *Science,* **305,** 1138–1140.

Kunkel, K. E., K. Andsager, and D. R. Easterling, 1999: Long-term trends in extreme precipitation events over the conterminous United States and Canada. *J. Climate,* **12,** 2515–2527.

Lawrence, D. M., P. E. Thornton, K. W. Oleson, and G. B. Bonan, 2007: The partitioning of evapotranspiration into transpiration, soil evaporation, and canopy evaporation in a GCM: Impacts on land–atmosphere interaction. *J. Hydrometeor.,* **8,** 862–880.

Lawrimore, J. H., and T. C. Peterson, 2000: Pan evaporation trends in dry and humid regions of the United States. *J. Hydrometeor.,* **1,** 543–546.

LeMone, M. A., R. L. Grossman, F. Chen, K. Ikeda, and D. Yates, 2003: Choosing the averaging interval for comparison of observed and modeled fluxes along aircraft transects over a heterogeneous surface. *J. Hydrometeor.,* **4,** 179–195.

Lettenmaier, D. P., A. W. Wood, R. N. Palmer, E. F. Wood, and E. Z. Stakhiv, 1999: Water resources implications of global warming: A U.S. regional perspective. *Climatic Change,* **43,** 537–579.

Liepert, B. G., 2002: Observed reductions of surface solar radiation at sites in the United States and worldwide from 1961 to 1990. *Geophys. Res. Lett.,* **29,** 1421, doi:10.1029/2002GL014910.

Lins, H. F., and J. R. Slack, 1999: Streamflow trends in the United States. *Geophys. Res. Lett.,* **26,** 227–230.

Liu, B., M. Xu, M. Henderson, and W. Gong, 2004: A spatial analysis of pan evaporation trends in China, 1955–2000. *J. Geophys. Res.,* **109,** D15102, doi:10.1029/2004JD004511.

Margulis, S. A., E. F. Wood, and P. A. Troch, 2006: The terrestrial water cycle: Modeling and data assimilation across catchment scales. *J. Hydrometeor.,* **7,** 309–311.

McCabe, G. J., and D. M. Wolock, 2002: Trends and temperature sensitivity of moisture conditions in the conterminous United States. *Climate Res.,* **20,** 19–29.

Mesinger, F., and Coauthors, 2006: North American regional reanalysis. *Bull. Amer. Meteor. Soc.,* **87,** 343–360.

Milly, P. C. D., and K. A. Dunne, 2001: Trends in evaporation and surface cooling in the Mississippi River basin. *Geophys. Res. Lett.,* **28,** 1219–1222.

Mitchell, T. D., T. R. Carter, P. D. Jones, M. Hulme, and M. New, 2004: A comprehensive set of high-resolution grids of monthly climate for Europe and the globe: The observed record (1901–2000) and 16 scenarios (2001–2100). Tyndall Centre Working Paper 55, 30 pp. [Available online at http://www.tyndall.ac.uk/publications/working_papers/wp55_summary.shtml.]

New, M., M. Hulme, and P. Jones, 1999: Representing twentieth-century space–time climate variability. Part I: Development of a 1961–90 mean monthly terrestrial climatology. *J. Climate,* **12,** 829–856.

Nigam, S., and A. Ruiz-Barradas, 2006: Seasonal hydroclimate variability over North America in global and regional reanalyses and AMIP simulations: Varied representation. *J. Climate,* **19,** 815–837.

Niu, G.-Y., Z.-L. Yang, R. E. Dickinson, and L. E. Gulden, 2005: A simple TOPMODEL-based runoff parameterization (SIMTOP) for use in global climate models. *J. Geophys. Res.,* **110,** D21106, doi:10.1029/2005JD006111.

——, ——, ——, ——, and H. Su, 2007: Development of a simple groundwater model for use in climate models and evaluation with Gravity Recovery and Climate Experiment data. *J. Geophys. Res.,* **112,** D07103, doi:10.1029/2006JD007522.

Ohmura, A., and M. Wild, 2002: Is the hydrological cycle accelerating? *Science,* **298,** 1345–1346.

Oleson, K. W., and Coauthors, 2004: Technical description of the community land model (CLM). NCAR Tech. Note NCAR/TN-461+STR, 186 pp.

Peterson, T. C., and R. S. Vose, 1997: An overview of the Global Historical Climatology Network temperature database. *Bull. Amer. Meteor. Soc.,* **78,** 2837–2849.

——, V. S. Golubev, and P. Ya. Groisman, 1995: Evaporation losing its strength. *Nature,* **377,** 687–688.

Philipona, R., and B. Dürr, 2004: Greenhouse forcing outweighs decreasing solar radiation driving rapid temperature rise over land. *Geophys. Res. Lett.,* **31,** L22208, doi:10.1029/2004GL020937.

——, ——, C. Marty, A. Ohmura, and M. Wild, 2004: Radiative forcing-measured at Earth's surface-corroborate the increasing greenhouse effect. *Geophys. Res. Lett.,* **31,** L03202, doi:10.1029/2003GL018765.

Qian, T., A. Dai, K. E. Trenberth, and K. W. Oleson, 2006: Simulation of global land surface conditions from 1948 to 2004. Part I: Forcing data and evaluation. *J. Hydrometeor.,* **7,** 953–975.

Rodell, M., and Coauthors, 2004: The Global Land Data Assimilation System. *Bull. Amer. Meteor. Soc.,* **85,** 381–394.

Roderick, M. L., and G. D. Farquhar, 2002: The cause of decreased pan evaporation over the past 50 years. *Science,* **298,** 1410–1411.

Schwartz, R. D., 2005: Global dimming: Clear-sky atmospheric transmission from astronomical extinction measurements. *J. Geophys. Res.,* **110,** D14210, doi:10.1029/2005JD005882.

Seneviratne, S. I., D. Lüthi, M. Litschi, and C. Schär, 2006: Land–atmosphere coupling and climate change in Europe. *Nature,* **443,** 205–209.

Stanhill, G., and S. Cohen, 2001: Global dimming: A review of the evidence for a widespread and significant reduction in global radiation with discussion of its probable causes and possible agricultural consequences. *Agric. For. Meteor.,* **107,** 255–278.

Sun, B., 2003: Cloudiness over the contiguous United States: Contemporary changes observed using ground-based and ISCCP D2 data. *Geophys. Res. Lett.,* **30,** 1053, doi:10.1029/2002GL015887.

Thomas, A., 2000: Spatial and temporal characteristics of potential evapotranspiration trends over China. *Int. J. Climatol.,* **20,** 381–396.

Trenberth, K. E., and D. J. Shea, 2005: Relationships between precipitation and surface temperature. *Geophys. Res. Lett.,* **32,** L14703, doi:10.1029/2005GL022760.

Vörösmarty, C. J., B. M. Fekete, M. Meybeck, and R. B. Lammers, 2000: Global system of rivers: Its role in organizing continental land mass and defining land-to-ocean linkages. *Global Biogeochem. Cycles,* **14,** 599–621.

Walter, M. T., D. S. Wilks, J.-Y. Parlange, and R. L. Schneider, 2004: Increasing evapotranspiration from the conterminous United States. *J. Hydrometeor.,* **5,** 405–408.

Wild, M., A. Ohmura, H. Gilgen, and D. Rosenfeld, 2004: On the consistency of trends in radiation and temperature records and implications for the global hydrological cycle. *Geophys. Res. Lett.,* **31,** L11201, doi:10.1029/2003GL019188.

Wu, W., and R. E. Dickinson, 2005: Warm-season rainfall variability over the U.S. Great Plains and its correlation with evapotranspiration in a climate simulation. *Geophys. Res. Lett.,* **32,** L17402, doi:10.1029/2005GL023422.

Yang, D., D. Kane, Z. Zhang, D. Legates, and B. Goodison, 2005: Bias corrections of long-term (1973–2004) daily precipitation data over the northern regions. *Geophys. Res. Lett.,* **32,** L19501, doi:10.1029/2005GL024057.

Zhang, Y. C., W. B. Rossow, and A. A. Lacis, 1995: Calculation of surface and top of atmosphere radiative fluxes from physical quantities based on ISCCP data sets. 1. Method and sensitivity to input data uncertainties. *J. Geophys. Res.,* **100,** 1149–1165.